A Mechanistic Model for Carbon Dioxide Corrosion of Mild Steel in the Presence of Protective Iron Carbonate Films—Part 2: A Numerical Experiment

S. Nešić,[‡,]* M. Nordsveen,** R. Nyborg,*** and A. Stangeland****

ABSTRACT

A theoretical carbon dioxide (CO₂) corrosion model was used to conduct numerical experiments, which allowed total insight into the underlying physicochemical processes. The focus was on factors influencing protective iron carbonate film formation and the effect that these films have on the CO₂ corrosion process. It was confirmed that high bulk pH, high temperature, high partial pressure of CO₂, high Fe²⁺ concentration, and low velocity all lead to favorable conditions for protective iron carbonate film formation. The model can be used to identify threshold values of these parameters. Corrosion rate was not strongly correlated with protective film thickness. The so-called surface film "coverage" effect appeared to be more important. Corrosion rates decreased rapidly as the film density increased. It was shown that in the presence of dense films diffusion of dissolved CO₂ through the film is the main mechanism of providing the reactants to the corrosion reaction at the metal surface. It was demonstrated that "detached" films have poor protective properties even when they are very dense. Serious errors in prediction/ reasoning can be made by operating with bulk instead of surface water chemistry conditions. The former is made

---

possible by using advanced models such as the one used in the present study.

KEY WORDS: carbon dioxide, carbon dioxide corrosion, carbon steel, model, prediction, protective films

INTRODUCTION

A theoretical model such as the one presented in Part 1 of this study[1] can be used to conduct numerical experiments (i.e., to vary different parameters and observe the effects they have on the corrosion process). This can be done easily, inexpensively, and with a total insight into the underlying physico-chemical processes—something that is difficult to achieve in real experiments. A numerical study of key parameters affecting protective iron carbonate film formation in carbon dioxide (CO₂) corrosion is presented. Subsequently, the model was used to investigate the ways in which these films reduce CO₂ corrosion rates.

From experimental evidence[2-4] it seems clear that rates of CO₂ corrosion can be reduced significantly when iron carbonate film precipitates on the surface of the steel. The overall reaction is:

$$Fe^{2+} + CO_3^{2-} \Rightarrow FeCO_3 \qquad (1)$$
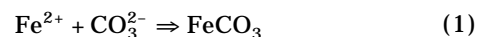
Precipitation will occur when concentrations ($c_{Fe^{2+}}$ and $c_{CO_3^{2-}}$) exceed the solubility product (K_{sp}), which is a function of temperature and ionic strength. In most cases, nucleation, which is the initial stage of precipitation, can be disregarded, and it can be assumed

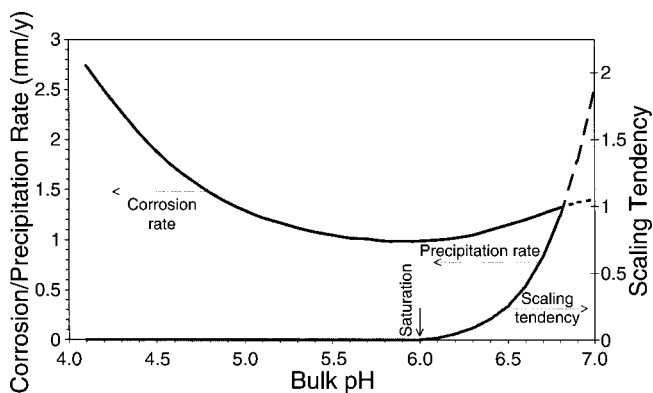**FIGURE 1.** *Effect of pH on corrosion rate, precipitation rate, and scaling tendency for T = 20°C, p_{CO_2} = 1 bar, $c_{Fe^{2+}}$ = 1 ppm, v = 1 m/s, and d = 0.01 m.*

that the rate of precipitation is controlled by the crystal growth rate. Many theories describing the mechanism and kinetics of crystalline film growth lead to a quadratic dependence on supersaturation:[5]

$$R_{gr} = k_{gr}(S - 1)^2 \qquad (2)$$

where R_{gr} is the growth rate, k_{gr} is the growth rate constant, and supersaturation is defined as:

$$S = \frac{c_{Fe^{2+}} c_{CO_3^{2-}}}{K_{sp}} \qquad (3)$$

From the two different relations for the kinetics of precipitation built into the model,[1] only the one proposed by van Hunnik, et al.,[6] will be used in the following discussion, as it is believed to yield more realistic results particularly at higher supersaturations.

To get appreciable rates of precipitation, supersaturation (S) has to be significantly larger than unity and the kinetic constant (k_{gr}) has to be large. Protective iron carbonate films have been observed in systems with high Fe^{2+} concentrations, high p_{CO_2}, and pH >5, which all lead to high S, and at high temperature, which leads to high k_{gr}. Actually, at room temperature, little or no iron carbonate film forms even at high supersaturations as a result of the slow kinetics of the precipitation reaction (low k_{gr}) but also attributable to the fact that the metal surface "corrodes away" under the film. The latter process has been quantified through the use of a nondimensional parameter termed "scaling tendency":[6]

---

[1] The choice of these parameters was indeed arbitrary; however, the reasons behind selecting the particular set of values will become obvious as the argument develops in the subsequent text. Throughout the text, solution properties such as pH, temperature, etc., always refer to the bulk unless it is explicitly stated otherwise.

$$ST = \frac{R_{gr}}{CR} \qquad (4)$$

which describes the relative rates of precipitation and corrosion prior to any film formation expressed in the same volumetric units. Obviously for ST<<1 the rapidly corroding metal surface opens voids under the film much faster than precipitation can fill them out, leading to porous and unprotective films. As ST exceeds, unity conditions become favorable for formation of dense protective iron carbonate films. The rate of precipitation has also a bearing on the morphology of the films formed;[5] however, this factor has not been accounted for in the present version of the model.

The mechanistic model described in Part 1 of this study[1] is an ideal platform for testing the concepts presented above as it provides a detailed description of a corroding system, which includes complete species concentration fields in time and space. Most of the previously published models were based on the bulk water chemistry conditions, which can be very different to the conditions at the metal surface where films form, as will be demonstrated. With the aid of the present model,[1] the rate of precipitation and the scaling tendency can be computed easily at the metal surface—called below *surface scaling tendency* (SST)—for any given set of environmental conditions.

RESULTS

In this section, a number of different corrosion scenarios have been explored. Initially, conditions affecting film formation are investigated such as temperature, pH, p_{CO_2}, Fe^{2+} concentration, and velocity. Subsequently, the role of protective films in reducing CO_2 corrosion is investigated with particular focus on the effects of film thickness, porosity, and morphology.

Factors Affecting Film Formation

Effect of pH — It is well accepted that to form iron carbonate films in CO_2 corrosion, the pH has to exceed a critical value, which depends on temperature, Fe^{2+} concentration, ionic strength, etc. Above the critical pH, saturation is exceeded and precipitation starts. To simplify the analysis, the following initial test case was selected:[1] temperature (T) = 20°C, partial pressure of CO_2 (p_{CO_2}) = 1 bar, dissolved ferrous ion concentration ($c_{Fe^{2+}}$) = 1 ppm, velocity (v) = 1 m/s, and pipe diameter (d) = 0.01 m. For this set of environmental conditions, the predicted effect of bulk pH on the corrosion rate is shown in Figure 1. The observed reduction of the corrosion rate between pH 4 and pH 6 is related to the general depletion of the H^+ ions, which are required for one of the two possible cathodic reactions: hydrogen reduction or direct

reduction of carbonic acid (H_2CO_3). At pH 6, practically the complete cathodic current is provided by the latter reaction. The reason that the model predicts a slight rise in the corrosion rate above bulk pH 6 is related to the inverse dependence of H_2CO_3 reduction on pH as described elsewhere.[7] More importantly, at bulk pH 6 the surface concentration of Fe^{2+} and CO_3^{2-} exceeds the solubility limit and precipitation of iron carbonate is initiated. Nevertheless, it is not very likely that any dense protective films can form below bulk pH 6.8, a point where the precipitation rate "catches up" with the corrosion rate and any "gaps" created by corrosion can be "filled up" by the precipitated film. At this point the SST = 1. Beyond pH 6.8, where the SST >1, it is likely that protective films would eventually form and alter both the corrosion and the precipitation rate calculated without a film present. Therefore, for SST >1, the predictions made in the present simulations done without any films are shown only tentatively as dashed lines. Corrosion data obtained from experimental investigation support, at least qualitatively, the above arguments as it has been found frequently that in laboratory experiments at 20°C iron carbonate films form very slowly, and a high pH and very long exposure times are required to form protective films.

The profile of supersaturation as a function of distance from the metal surface for different bulk pH shown in Figure 2 illustrates the error in prediction/reasoning, which can be made by operating with bulk instead of surface water chemistry conditions. It can be seen that based on the bulk pH one could conclude that precipitation would not begin below bulk pH 6.6, whereas at the surface of the steel the saturation is approached already at bulk pH 6.0. The supersaturation profiles in Figure 2 are calculated from the concentration profiles for the Fe^{2+} and CO_3^{2-} species and pH. An example is shown in Figure 3 where all the main dissolved species concentrations are shown as a function of distance from a corroding steel surface at bulk pH 6.3. At the surface, pH 6.7 is achieved as a result of the corrosion process—what reduces the solubility of iron carbonate and consequently increases the level of supersaturation. This is aided by increased concentrations of Fe^{2+} and CO_3^{2-} at the surface. All the concentrations in Figure 3 are shown as deviation from the bulk equilibrium conditions to avoid a broad disparity of scales.[(2)]

Effect of Temperature — In numerous laboratory mild steel CO_2 corrosion studies, it has been reported that in order to obtain protective iron carbonate films in reasonably short time frames, the temperature has to be elevated above room temperature (or the pH must be much higher than 6). The temperature effect is illustrated in Figure 4 for the case of corrosion in a

FIGURE 2. *Difference between the bulk and surface conditions at different pH for T = 20°C, p_{CO_2} = 1 bar, $c_{Fe^{2+}}$ = 1 ppm, v = 1 m/s, and d = 0.01 m.*
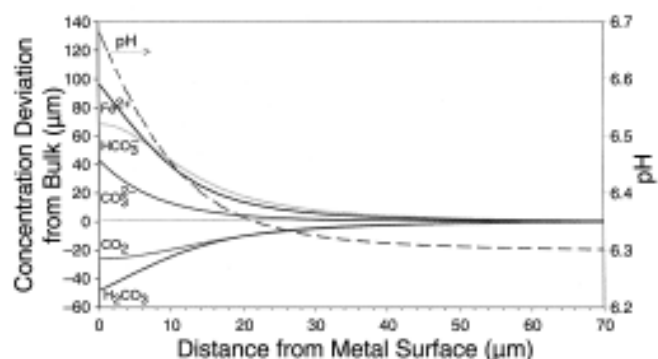
FIGURE 3. *Concentration profiles for the main dissolved species in the CO_2 solution shown as the deviation from the bulk equilibrium conditions for T = 20°C, bulk pH 6.3, p_{CO_2} = 1 bar, $c_{Fe^{2+}}$ = 1 ppm, v = 1 m/s, and d = 0.01 m.*

FIGURE 4. *Effect of temperature on corrosion and precipitation rates for pH 6, p_{CO_2} = 1 bar, $c_{Fe^{2+}}$ = 1 ppm, v = 1 m/s, and d = 0.01 m.*

CO_2 solution at pH 6, p_{CO_2} = 1 bar, $c_{Fe^{2+}}$ = 1 ppm, v = 1 m/s, and d = 0.01 m. At this pH, saturation is exceeded at the surface even at 20°C, as illustrated in Figure 2. However, any protective film formation is unlikely at this low temperature since the SST <<1, as shown in Figure 1. As the temperature is increased above 50°C, with all other parameters un-

---

[(2)] For this particular case, the bulk concentrations of dissolved CO_2 and HCO_3^- are on the order of 10^{-2} M while concentrations of H_2CO_3, CO_3^{2-}, and Fe^{2+} are on the order of 10^{-5} M.
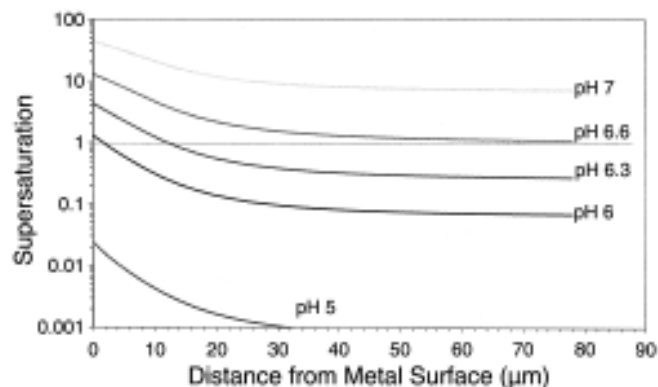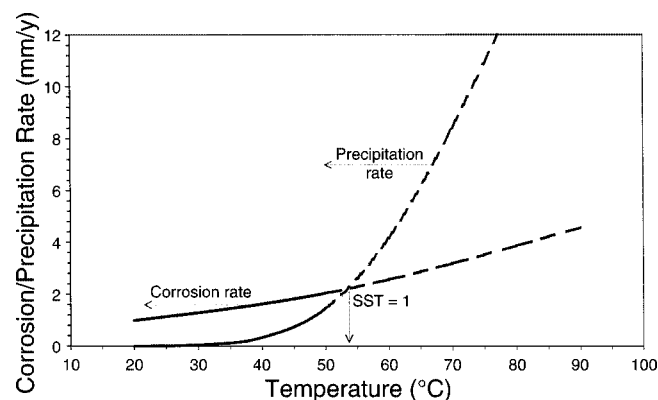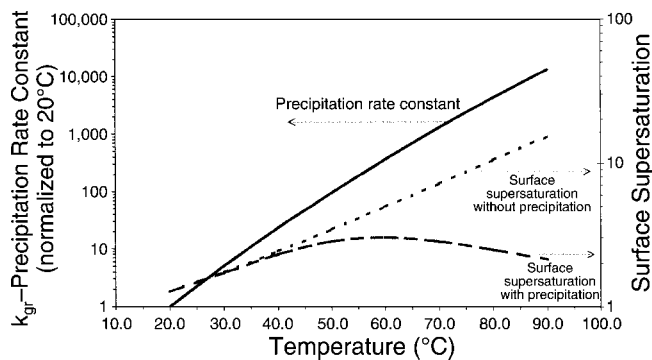
FIGURE 5. *Effect of temperature on the precipitation constant (k_{gr}) and surface supersaturation for pH 6, p_{CO_2} = 1 bar, c_{Fe2+} = 1 ppm, v = 1 m/s, and d = 0.01 m.*
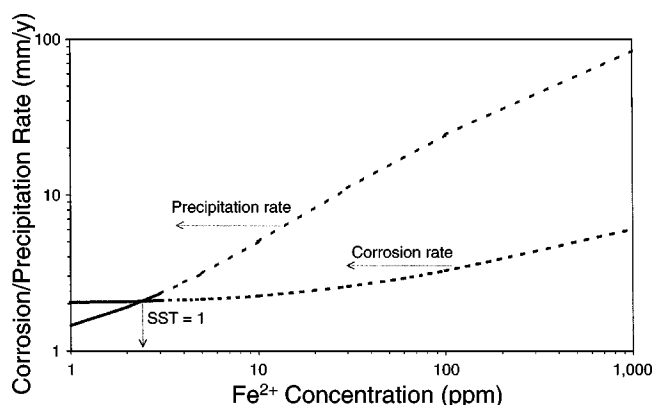

FIGURE 6. *Effect of Fe^{2+} concentration on the corrosion and precipitation rates for pH 6, T = 60°C, p_{CO_2} = 1 bar, v = 1 m/s, and d = 0.01 m.*

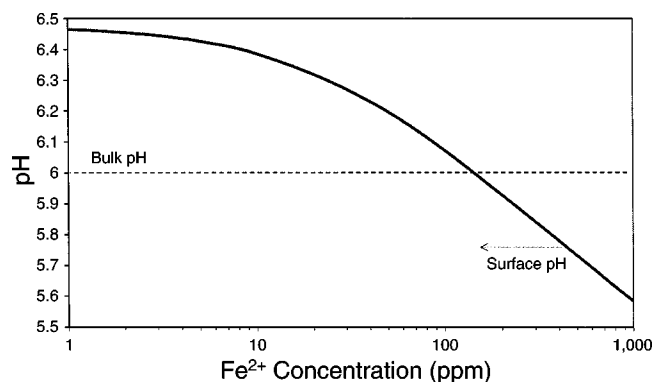**FIGURE 7.** *Effect of Fe^{2+} concentration pH at the surface for pH 6, T = 60°C, p_{CO_2} = 1 bar, v = 1 m/s, and d = 0.01 m.*

changed, SST approaches and exceeds unity, suggesting that protective film formation is likely. The reason for this behavior, which qualitatively matches experimental observations, lies in the increased rate of the precipitation as expressed by the precipitation rate "constant" k_{gr}. The model of van Hunnik, et al.,[6] predicts a thousandfold increase in k_{gr} as the tem-

perature is increased from 20°C to 70°C, as shown in Figure 5. It is interesting to observe from the same figure that even at high temperatures where the solubility of iron carbonate is low, the surface supersaturation is <3. The reason for this is the fast precipitation process, which depletes the surface layer of Fe^{2+} and CO_3^{2-} ions maintaining a relatively low supersaturation. When precipitation is excluded from the model, three to four times larger surface supersaturation is obtained, as illustrated in Figure 5. It is worth noting that at the same time the bulk supersaturation stays well below unity over the whole range of temperatures studied, once again illustrating a possible source of error, which can be made by operating exclusively with bulk conditions.

Effect of Fe^{2+} Concentration — Another well-established factor that leads to faster and denser film formation is the increase in the concentration of Fe^{2+} ions in the solution. By looking at Equation (3), it is clear that increased c_{Fe2+} gives higher supersaturation (S) and this in turn leads to a higher precipitation rate (R_{gr}) as given by Equation (2) and higher scaling tendency (ST) as defined by Equation (4).

To investigate the effect of Fe^{2+} concentration, a test case at T = 50°C, pH 6, p_{CO_2} = 1 bar, v = 1 m/s, and d = 0.01 m was selected. The results shown in Figure 6 indicate that under these conditions, as c_{Fe2+} is increased >2 ppm, the SST approaches and exceeds unity and formation of protective films is likely. In most closed laboratory systems (glass cells, autoclaves, and flow loops), rise of c_{Fe2+} in the solution is almost inevitable unless special measures are taken to remove Fe^{2+}. However, in once-through systems found in practice, and particularly in gas-condensate systems involving high rates of condensation, c_{Fe2+} may never reach the critical value.

Very often in laboratory experiments large amounts of Fe^{2+} are released into the solution in an effort to accelerate protective film formation. This does increase the rate of precipitation at the surface (Figure 6); however, the rate of corrosion temporarily increases as well, at least until some protective films form. This may seem odd, but calculations show that rapid precipitation at the surface occurring at very high c_{Fe2+} can lead to a reduction of the surface pH compared to the bulk pH and an increased corrosion rate. This is clearly shown in Figure 7 where for c_{Fe2+} < 100 ppm, surface pH is higher than bulk pH; however, for c_{Fe2+} > 200 ppm, mild "acidification" at the surface is obtained. Clearly in this case any simple calculations based on a bulk pH or even a surface pH, which is assumed to be larger than the bulk pH, can be in error.

Effect of CO_2 Partial Pressure — Frequently in simple CO_2 corrosion experiments it is difficult to obtain protective iron carbonate films in a reasonably short period—typical experiments last a few days at most. In an effort to achieve rapid film formation,

temperature is often increased to >50°C to accelerate the kinetics of precipitation. It is frequently overlooked that this is always accompanied by a significant increase in water vapor partial pressure (p_v). Given that the total pressure (p) in the experiments remains constant (atmospheric), and that:

$$p = p_{CO_2} + p_v \qquad (5)$$

then, with the increase in temperature, the partial pressure of CO_2 in the gas phase (p_{CO_2}) decreases (Figure 8). Correspondingly, the amount of dissolved CO_2 in water also decreases, following Henry's law. Therefore, for a given pH, the concentration of carbonic species including CO_3^{2-} is also reduced. By inspecting Equations (2) and (3), it becomes clear that the increase in temperature in an experiment operating at atmospheric pressure will give rise to two opposing effects. On one hand, an increase in the kinetics of precipitation will occur since k_{gr} increases with temperature (Figure 5). On the other hand, a reduction of supersaturation (S) will happen as a result of a lesser amount of CO_2 dissolved in water at higher temperatures. To clarify which effect prevails, the corrosion and precipitation rates are shown in Figure 8 for a range of temperatures for a given total pressure of 1 bar and pH 6, $c_{Fe^{2+}} = 1$ ppm, $v = 1$ m/s, and d = 0.01 m. It can be seen that some precipitation starts already >30°C; however, protective films can be expected only >60°C when SST >> 1. This is in agreement with experimental observations where in the majority of glass cell experiments targeting iron carbonate film formation it was found that the temperature needs to be >60°C. The actual values shown in Figure 8 will vary somewhat with pH, $c_{Fe^{2+}}$, and velocity; however, the overall behavior will remain the same.

Autoclaves or flow loops are used to investigate corrosion at higher CO_2 partial pressures. The effect of increased CO_2 partial pressure (p_{CO_2}) on film formation is illustrated in Figure 9 for the case of CO_2 corrosion at T = 50°C, pH 6, $c_{Fe^{2+}} = 1$ ppm, v = 1 m/s, and d = 0.01 m. Clearly, for $p_{CO_2} \leq 1$ bar, the resulting precipitation will not be sufficient to form protective films. On the other hand, when $p_{CO_2} \geq 2$ bar, surface supersaturation increases leading to rapid precipitation and protective film formation (Figure 10). It is interesting to notice that as p_{CO_2} is increased the pH at the surface initially increases due to corrosion and release of Fe^{2+} ions, and then decreases due to rapid precipitation as shown in Figure 10. It appears that this trend would continue to even higher p_{CO_2}; however, as the model was never calibrated against very high p_{CO_2} data, its use in this domain would be unreliable.

In summary, although it is generally true that CO_2 corrosion becomes more aggressive at higher CO_2 partial pressures, the rate of precipitation also
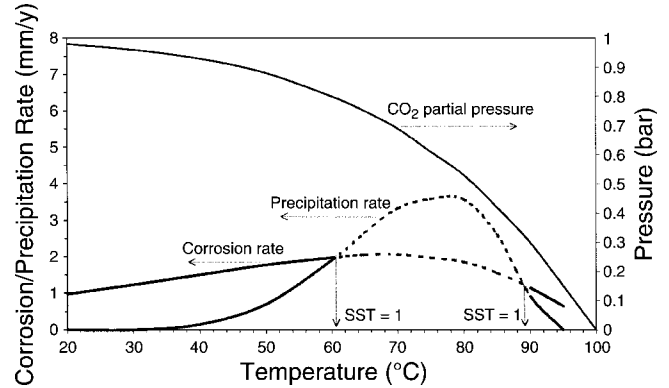

FIGURE 8. *Effect of temperature on CO_2 partial pressure, corrosion rate, and precipitation rate in a glass cell experiment conducted at 1 bar total pressure for pH 6, $c_{Fe^{2+}} = 1$ ppm, v = 1 m/s, and d = 0.01 m.*

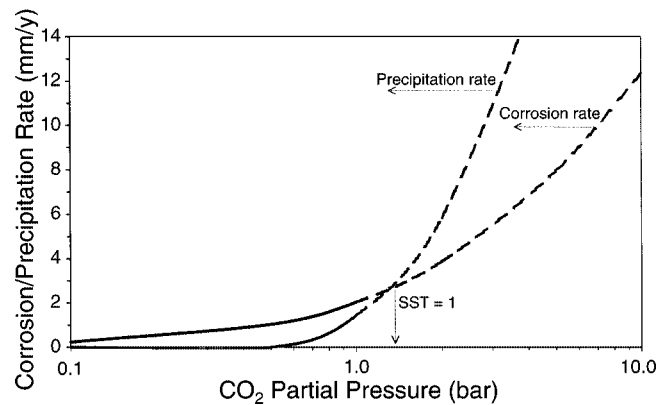**FIGURE 9.** *Effect of CO_2 partial pressure on the corrosion and precipitation rates for T = 50°C, pH 6, $c_{Fe^{2+}} = 1$ ppm, v = 1 m/s, and d = 0.01 m.*
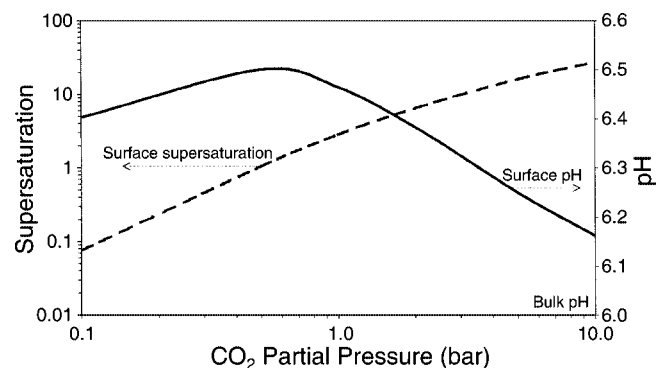

FIGURE 10. *Effect of CO_2 partial pressure on the surface supersaturation and surface pH for T = 50°C, pH 6, $c_{Fe^{2+}} = 1$ ppm, v = 1 m/s, and d = 0.01 m.*

increases. These simulations show that the rate of iron carbonate precipitation can increase faster than the corrosion rate with increasing CO_2 partial pressure (at constant pH). Consequently, it becomes easier to form protective iron carbonate films at high
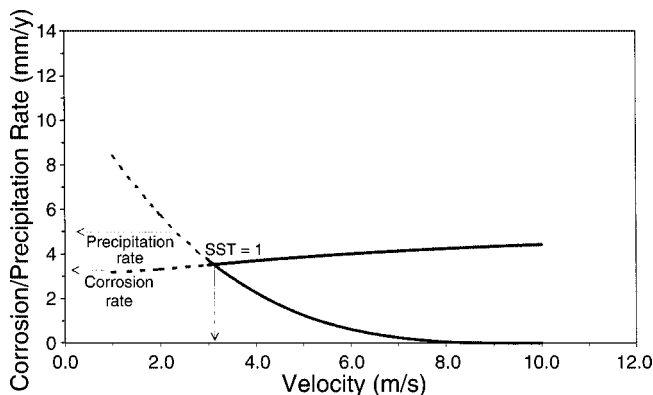
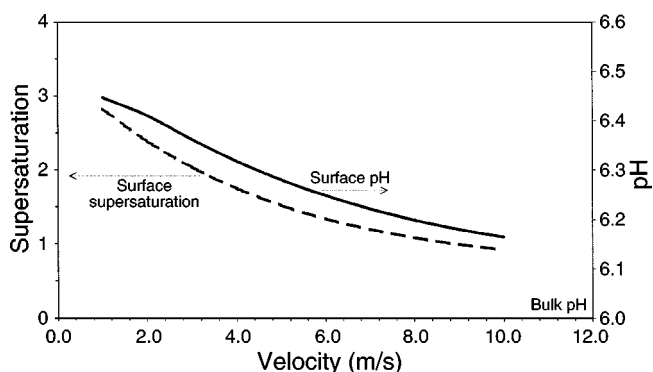**FIGURE 11.** *Effect of velocity on the corrosion and precipitation rates for T = 70°C, pH 6, p_{CO_2} = 1 bar, $c_{Fe^{2+}}$ = 1 ppm, and d = 0.01 m.*

FIGURE 12. *Effect of velocity on surface supersaturation and surface pH for T = 70°C, bulk pH 6, p_{CO_2} = 1 bar, $c_{Fe^{2+}}$ = 1 ppm, and d = 0.01 m.*

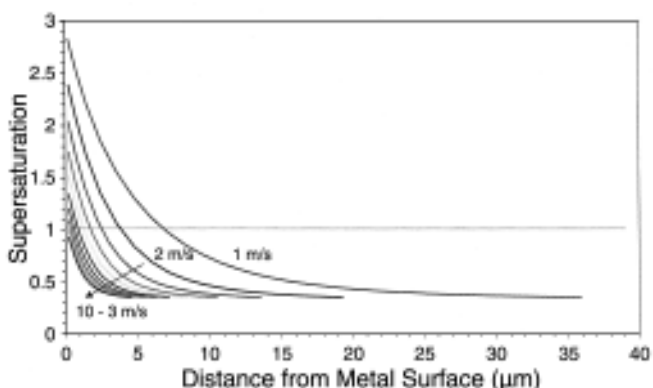**FIGURE 13.** *Profile of super-/under-saturation as a function of distance from the wall for T = 70°C, bulk pH 6, p_{CO_2} = 1 bar, $c_{Fe^{2+}}$ = 1 ppm, and d = 0.01 m.*

CO_2 partial pressure, resulting in a reduction of the corrosion rate.

Effect of Velocity — Velocity affects corrosion in a number of ways. Once the films are in place it can contribute to their removal by mechanical means (erosion), chemical means (dissolution), or a combination of the two. On the other hand, it also affects

film-free corrosion by altering the mass transfer of dissolved species toward and away from the surface. The latter effect, as related to film formation, will be discussed.

The effect of velocity has been explored by looking at the following test case: T = 70°C, pH 6, p_{CO_2} = 1 bar, $c_{Fe^{2+}}$ = 1 ppm, and d = 0.01 m. For these conditions, it can be seen from Figure 11 that the corrosion rate does not depend significantly on velocity primarily because of the high pH when the corrosion rate is predominantly controlled by charge transfer. On the other hand, the precipitation rate drops rapidly with increased velocity. At low velocities, the rate of precipitation at the surface is much higher than the rate of corrosion (leading to a high scaling tendency), which tends to suggest rapid protective film formation. Above a threshold value, formation of protective films seems unlikely. The explanation is easily deduced by looking at Figure 12, where with increased velocity, the surface pH and consequently surface supersaturation are shown to steadily decrease, approaching the value in the bulk. Clearly, this is a consequence of the thinning of the mass-transfer boundary layer. In other words, higher velocity and higher near-wall turbulence levels associated with it promote more efficient mixing nearer to the wall, which results in Fe^{2+} ions being swept away from the wall before they can precipitate to form a film. For the particular case discussed, this is illustrated in Figure 13 where the level of saturation is shown as a function of distance from a corroding surface. The thickness of the boundary layer, as well as the difference between the surface and bulk saturation, decrease as the velocity is increased. For velocities >3 m/s, the scaling tendency falls below 1 (Figure 11) and protective film formation is unlikely. From Figure 13, it also can be seen that the solution near the surface becomes unsaturated at >10 m/s and all precipitation at the surface stops (and dissolution starts).

CO_2 Corrosion in the Presence of Surface Films

The analysis presented focused on the conditions that affect film formation. The model of film growth is still under development. However, the present model allows corrosion behavior to be analyzed in the presence of films once the properties of the film, such as thickness, porosity, and morphology, are defined in advance.

Effect of Film Thickness — It is commonly accepted that when macroscopic protective surface films (scales) are present they retard corrosion by behaving as a diffusion barrier for species involved in the corrosion reaction. This does not apply to the very thin, often invisible passive films but rather to much thicker corrosion films or scales. In other words, the porous surface films make it more difficult for the species to move to and away from the

surface, as they have to find their way through a tangled maze of pores in the film. This implies that the thicker the films are, the more protective they should become as the path needed to be covered by the diffusing species becomes longer. This simple idea, which clearly applies to single-species diffusion (e.g., in oxygen corrosion), was tested here for the more complicated case of CO_2 corrosion where there are many diffusing species and a number of chemical reactions between them can occur.

The results shown in Figure 14 for the case of CO_2 corrosion in the presence of a film with 30% porosity at T = 50°C, pH 6, p_{CO_2} = 2 bar, $c_{Fe^{2+}}$ = 1 ppm, and d = 0.01 m did not confirm the simplistic expectations about the effect of film thickness.[3] It can be seen that the corrosion rate changed only slightly as the thickness of the film was increased. The explanation for this behavior is given in the following section where the effects of porosity and transport of species are analyzed in detail. From Figure 14 it also can be seen that the corrosion rate was reduced even in the presence of extremely thin films, suggesting the importance of the so-called surface "coverage" effect, when a portion of the surface under the film becomes "unavailable" for corrosion. This implies that electrochemical reactions do not occur at the locations of the surface where the film is attached to the metal.

It should also be noted that the scaling tendency, which in this case indicates the likelihood of the existing film pores to fill up further with the precipitate, initially decreases sharply as the film starts forming on the surface and then increases. This complicated behavior, which will be elucidated in the following section, does suggest that thin, porous, and only slightly protective films do not always lead to formation of denser, more protective films.

It is also worth mentioning that the predicted lack of correlation of film thickness and associated CO_2 corrosion rate has been confirmed during a recent analysis of a large number of experimental test cases for CO_2 corrosion in the presence of iron carbonate films. This analysis showed that film porosity is much more important than film thickness.

Effect of Film Porosity — The effect of film porosity is illustrated in Figure 15 for the case of a 50-µm-thick film and T = 50°C, pH 6, p_{CO_2} = 2 bar, $c_{Fe^{2+}}$ = 1 ppm, and d = 0.01 m. It can be seen that both the corrosion and precipitation rates decrease rapidly as the film density (the inverse of porosity) increases, as would be expected. This is mainly a result of a reduction in the flux of species, which "fuel" the respective electrochemical and chemical reactions. Nevertheless, in a system with so many species and reactions, it is not clear which species flux is affected and to what extent. To investigate this, the concentration
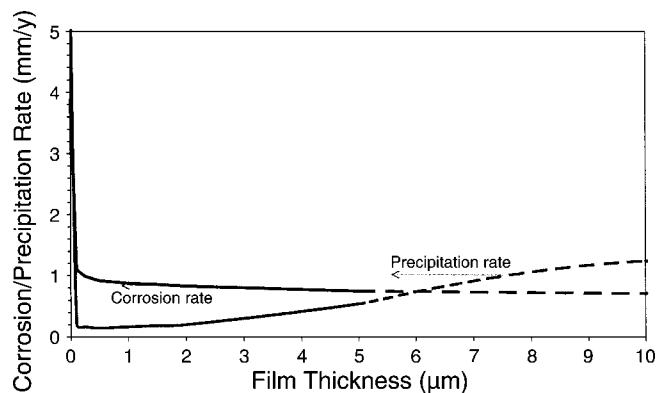

FIGURE 14. *Effect of film thickness on the corrosion and precipitation rates for T = 50°C, pH 6, p_{CO_2} = 2 bar, $c_{Fe^{2+}}$ = 1 ppm, and d = 0.01 m.*
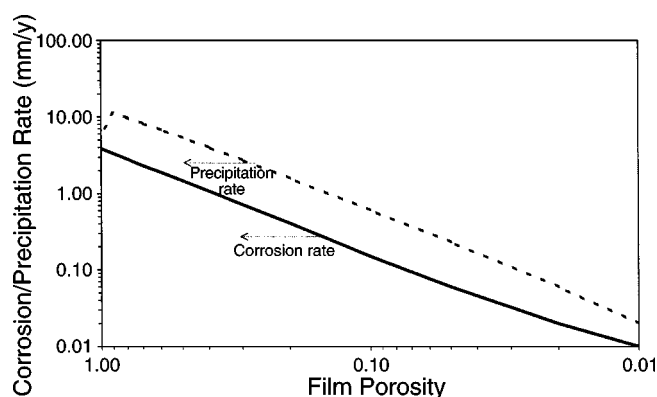

FIGURE 15. *Effect of film porosity on the corrosion and precipitation rates for a 50-µm-thick film and T = 50°C, pH 6, p_{CO_2} = 2 bar, $c_{Fe^{2+}}$ = 1 ppm, and d = 0.01 m.*
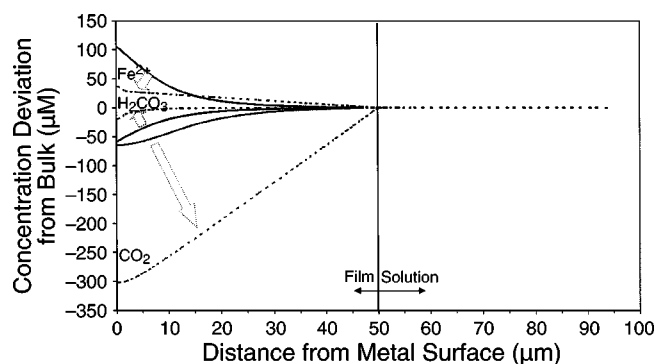

FIGURE 16. *Concentration profiles for the three main dissolved species present in the CO_2 solution shown as the deviation from the bulk equilibrium conditions. Full line (——) indicates the film-free conditions; dashed lines (- - - -) indicates concentrations in the presence of a 50-µm-thick film with a 1% porosity. Other conditions: T = 50°C, pH 6, p_{CO_2} = 2 bar, $c_{Fe^{2+}}$ = 1 ppm, and d = 0.01 m.*

profiles for the three of the main species present in the solution are compared in Figure 16 for the cases of film-free corrosion and a 50-µm-thick, 99% "dense" (1% porous) film. It appears that in the presence of a dense film the concentrations of H_2CO_3 and
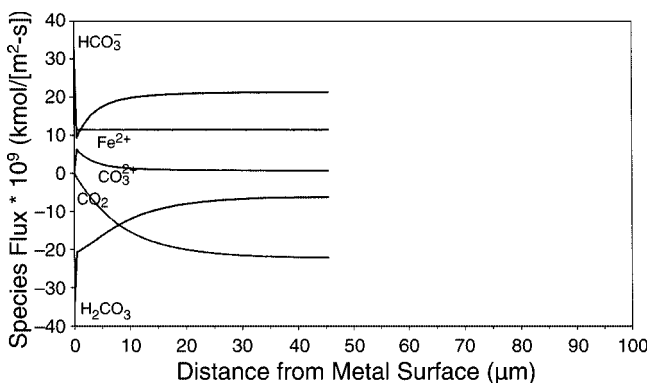
FIGURE 17. *Flux profiles for the main dissolved species present in the CO_2 solution shown for the case of film-free corrosion and T = 50°C, pH 6, p_{CO_2} = 2 bar, $c_{Fe^{2+}}$ = 1 ppm, and d = 0.01 m.*
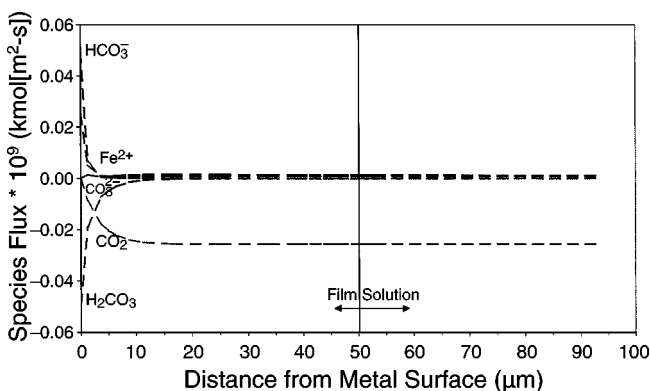

FIGURE 18. *Flux profiles for the main dissolved species present in the CO_2 solution shown for the case of a 50-μm-thick film with a 1% porosity, T = 50°C, pH 6, p_{CO_2} = 2 bar, $c_{Fe^{2+}}$ = 1 ppm, and d = 0.01 m.*
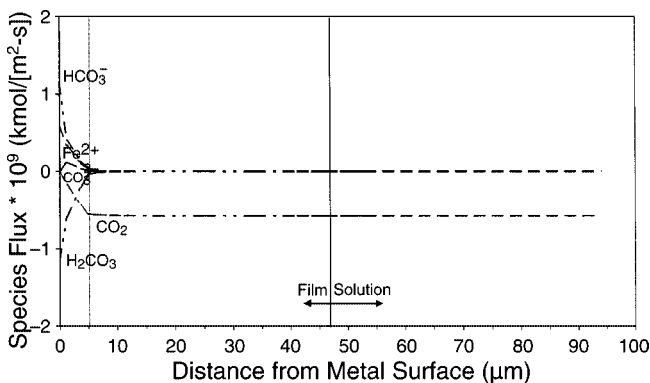

FIGURE 19. *Flux profiles for the main dissolved species present in the CO_2 solution shown for the case of a "detached" 50-μm-thick film. Porosity is 10% in the 5-μm-thick layer adjacent to the corroding surface and 1% in the remaining 45 μm. Other conditions: T = 50°C, pH 6, p_{CO_2} = 2 bar, $c_{Fe^{2+}}$ = 1 ppm, and d = 0.01 m.*

Fe^{2+} at the surface approach the bulk (equilibrium) conditions. The same is true for all the other species in the solution,[4] except for dissolved CO_2, which deviates significantly more from the bulk value compared to film-free corrosion. The explanation for this

behavior can be found by looking at the species flux plots for the two cases as shown in Figures 17 and 18. Clearly, in the presence of the dense film, all the fluxes are significantly reduced, as would be expected; however, the extent varies significantly. In the film-free case (Figure 17), all species have a similar magnitude flux (except for CO_3^{2-}, which is present in very small concentrations).

Importantly, only about a fifth of the H_2CO_3, which is consumed by the corrosion process as the main cathodic species, diffuses from the bulk through the mass-transfer boundary layer. The rest is "produced locally" by direct hydration of dissolved CO_2 in a layer near the corroding steel surface—often called the chemical reaction boundary layer. Conversely, in the case of a 50-μm-thick, 99% dense film, virtually all (99.9%) of the H_2CO_3 is produced locally in the thin chemical reaction boundary layer within the film. Outside this layer (throughout the rest of the film and in the mass-transfer boundary layer), the flux of all species other than dissolved CO_2 is very small, meaning that diffusion of dissolved CO_2 through the dense film is the main mechanism of providing the reactants to the corrosion reaction at the metal surface. This result appears as a consequence of a complex interplay between the rates of diffusion and chemical reactions involving the species present in the solution.

Effect of Film Morphology — Indeed, with a model such as the one used in the present study, a large number of film morphologies can be investigated with fascinating and often unexpected results. For illustration purposes, a case is shown below where a protective 50-μm-thick film is studied, which is "detached" from the corrosion surface. To simulate this, porosity of the film in the first 5 μm adjacent to the metal surface has been set to 10% (an unprotective film) while the rest of the film had a 1% porosity (dense and protective). These kinds of films are often seen in reality and are considered to have poor protective properties. Following a simple mass-transfer theory, this does not appear to be logical as the exact location of the diffusion barrier appears to be irrelevant, as long as it is in place.

When the CO_2 corrosion process was simulated under this "detached" 50-μm-thick protective film, all other conditions were assumed to be identical to the ones in the previous section, which discussed fully "attached" films: T = 50°C, pH 6, p_{CO_2} = 2 bar, $c_{Fe^{2+}}$ = 1 ppm, and d = 0.01 m.

Interestingly, the corrosion rate in the case of the "detached" film was predicted to be 0.13 mm/y, much higher than initially expected. Compared with the corrosion rates for "attached" films shown in Figure 15, it appears that the "detached" 1% porous film performed similarly to a nine-times-more porous

---

[4] Not shown in the figure for clarity.

"attached" film of the same thickness. In other words, the more porous layer adjacent to the metal surface rendered the rest of the film, which was very dense, unprotective. This agrees with empirical observations that detached films are not protective.[8] Further insight can be gained by looking at Figure 19, showing the flux profiles for the main dissolved species present in the solution in the case of the "detached" film. The character of the curves is similar to the ones shown in Figure 18 for the case of a protective "attached" film, except that the magnitudes of the fluxes are one order higher.

It is interesting to mention finally that when a reverse situation was simulated—a two-layered, 50-μm-thick film, with a thin (5 μm) protective layer next to the surface (1% porosity) and a thick (45 μm) unprotective film (10% porosity) on the outside—a corrosion rate on the order of 0.01 mm/y was obtained. All these results tend to suggest that the main effect of protective iron carbonate films in CO_2 corrosion is to cover the metal surface and make it unavailable for corrosion rather than present an effective diffusion barrier.

CONCLUSIONS

❖ In this numerical study, experimental observations were confirmed that high-bulk pH, high temperature, high partial pressure of CO_2, and high dissolved iron concentration typically contribute to rapid protective iron carbonate film formation.

❖ High pH contributes to protective film formation by reducing the film-free corrosion rate and increasing the precipitation rate (via decreased solubility and increased supersaturation). This leads to a rapid increase of scaling tendency with pH.

❖ High temperature and partial pressure of CO_2 lead to two opposing effects: an increase in the precipitation rate and an increase in the underlying corrosion rate. Above a threshold pH, this leads to faster formation of protective films while at lower pH the effect is opposite.

❖ Concentration of dissolved Fe^{2+} is an important parameter in iron carbonate protective film formation. Typically, Fe^{2+} concentration needs to be increased to >1 ppm to make formation of iron carbonate protective films likely.

❖ Increase of velocity typically leads to less favorable conditions for protective film formation. Threshold velocities can be identified above which formation of

protective films was unlikely and in some cases impossible.

❖ Serious errors in prediction/reasoning can be made by operating with bulk instead of surface water chemistry conditions. The former is made possible by using advanced models such as the one used in the present study.

❖ Corrosion rate was not strongly correlated with protective film thickness. Corrosion rates decreased rapidly as the film porosity decreased.

❖ It was shown that in the presence of dense films diffusion of dissolved CO_2 through the film is the main mechanism of providing the reactants to the corrosion reaction at the metal surface.

❖ Protective films reduce the corrosion rate primarily by blocking the metal surface rather than by reducing the diffusion of corrosive species.

❖ It was demonstrated that "detached" films have poor protective properties even when they are very dense.

REFERENCES

1. M. Nordsveen, S. Nešić, R. Nyborg, A. Stangeland, Corrosion 59, 5 (2003): p. 443.
2. A. Dugstad, "Mechanism of Protective Film Formation During CO_2 Corrosion of Carbon Steel," CORROSION/98, paper no. 31 (Houston, TX: NACE International, 1998).
3. R. Nyborg, "Initiation and Growth of Mesa Corrosion Attack During CO_2 Corrosion of Carbon Steel," CORROSION/98, paper no. 48 (Houston, TX: NACE, 1998).
4. R. Nyborg, A. Dugstad, "Mesa Corrosion Attack in Carbon Steel and 0.5% Chromium Steel," CORROSION/98, paper no. 29 (Houston, TX: NACE, 1998).
5. J.W. Mullin, Crystallization, 3rd ed. (Oxford, U.K.: Oxford Press, 1993).
6. E.W.J. van Hunnik, B.F.M. Pots, E.L.J.A. Hendriksen, "The Formation of Protective $FeCO_3$ Corrosion Product Layers in CO_2 Corrosion," CORROSION/96, paper no. 6 (Houston, TX: NACE, 1996).
7. S. Nešić, J. Postlethwaite, S. Olsen, Corrosion 52 (1996): p. 280.
8. J.-L. Crolet, N. Thevenot, S. Nešić: "Role of Conductive Corrosion Products on the Protectiveness of Corrosion Layers," CORROSION/96, paper no. 4 (Houston, TX: NACE, 1996).